

Electronic Supplementary Information

Zn(II) complex with 2-quinolinecarboxaldehyde selenosemicarbazone: synthesis, structure, interaction studies with DNA/HSA, molecular docking and caspase-8 and -9 independent apoptosis induction

Nenad R. Filipović^a, Snežana Bjelogrić^b, Aleksandar Marinković^c, Tatjana Ž. Verbić^d, Ilija N. Cvijetić^e, Milan Senčanski^f, Marko Rodić^g, Miroslava Vujčić^h, Dušan Sladić^d, Zlatko Striković^d, Tamara R. Todorović,^{d*} Christian D. Muller^{i,j*}

^a *Department of Chemistry and Biochemistry, Faculty of Agriculture, University of Belgrade, Nemanjina 6, Belgrade, Serbia;* ^b *National Cancer Research Center of Serbia, Pasterova 14, Belgrade, Serbia;* ^c *Faculty of Technology and Metallurgy, University of Belgrade, Karnegijeva 4, Belgrade, Serbia;* ^d *Faculty of Chemistry, University of Belgrade, Studentski trg 12-16, Belgrade, Serbia;* ^e *Innovation Center of the Faculty of Chemistry, University of Belgrade, Studentski trg 12-16, Belgrade, Serbia,* ^f *Center for Multidisciplinary Research, Institute of Nuclear Sciences Vinča, University of Belgrade, Belgrade, Serbia;* ^g *Department of Chemistry, Faculty of Sciences, University of Novi Sad, Trg Dositeja Obradovića 4, Novi Sad, Serbia;* ^h *Institute of Chemistry, Technology and Metallurgy, University of Belgrade, Njegoševa 12, Belgrade, Serbia;* ⁱ *Laboratoire d'Innovation Thérapeutique, UMR 7200, Faculté de Pharmacie, Université de Strasbourg, 67401 Illkirch, France;* ^j *Plateforme eBioCyt, Faculté de Pharmacie & Fédération Translationnelle de Médecine, Université de Strasbourg, 67401 Illkirch, France.*

*Corresponding authors:

Dr. Tamara R. Todorović
E-mail: tamarat@chem.bg.ac.rs
Tel: +381 11 3336-685
Fax: +381 11 2184-330

Dr. Christian D. Muller
E-mail: cdmuller@unistra.fr
Tel: +33-688285839
Fax: +33-368854310

Content

Figure S1. Experimental and theoretical FT-IR spectra of 1	4
Figure S2. ^1H NMR spectrum of 1 in $\text{DMSO}-d_6$	5
Figure S3. ^{13}C NMR spectrum of 1 in $\text{DMSO}-d_6$	5
Figure S4. COSY spectrum of 1	6
Figure S5. NOESY spectrum of 1	6
Figure S6. ^1H – ^{13}C HSQC spectrum of 1	7
Figure S7. ^1H – ^{13}C HMBC spectrum of 1	7
Figure S8. Superimposed ^1H and ^{13}C NMR spectra of Hqasesc and 1	8
Figure S9. Superimposed ^1H NMR spectra of freshly prepared sample of 1 and sample after 24 h	9
Figure S10. Cyclic voltammograms of Hqasesc, 1 , and 1 with addition of zinc perchlorate	9
Figure S11. UV/Vis spectra of Hqasesc in pH range 1.65–5.17 and determination of K_{a1} at 341 nm.	10
Figure S12. UV/Vis spectra of Hqasesc in pH range 5.17–11.91 and determination of K_{a2} at 365 nm	10
Figure S13. Packing diagram in the crystal structure of Hqasesc	11
Figure S14. Packing diagram in the crystal structure of 1	11
Figure S15. Sigmoidal dose-response curves with ED50 values for Hqasesc, 1 and CDDP on THP-1 and AsPC-1 cells	13
Figure S16. Stern-Volmer plot of F_0/F vs. $[\text{Q}]$ at three different temperatures	14
Figure S17. Modified Stern-Volmer plot for binding of 1 to HSA at three temperatures	14
Figure S18. The plot of $\ln K_a$ vs. $1/T$ for the interaction of 1 with HSA	15
Figure S19. Double-log plot for determination of binding constants K_b , and the number of binding sites n at three temperatures	15
Figure S20. Spectral overlap of the complex 1 absorption with HSA fluorescence emission	16
Figure S21. All conformations of 1 in the DNA duplex	16
Figure S22. Structure of HSA and the location of complex 1 binding site	17
Scheme S1. Numbering of atoms of Hqasesc in 1	4

Table S1. Hydrogen bonding geometry (Å, °) in Hqasesc and 1	12
Table S2. Interactions of HSA binding site atoms with 1	18
References	18

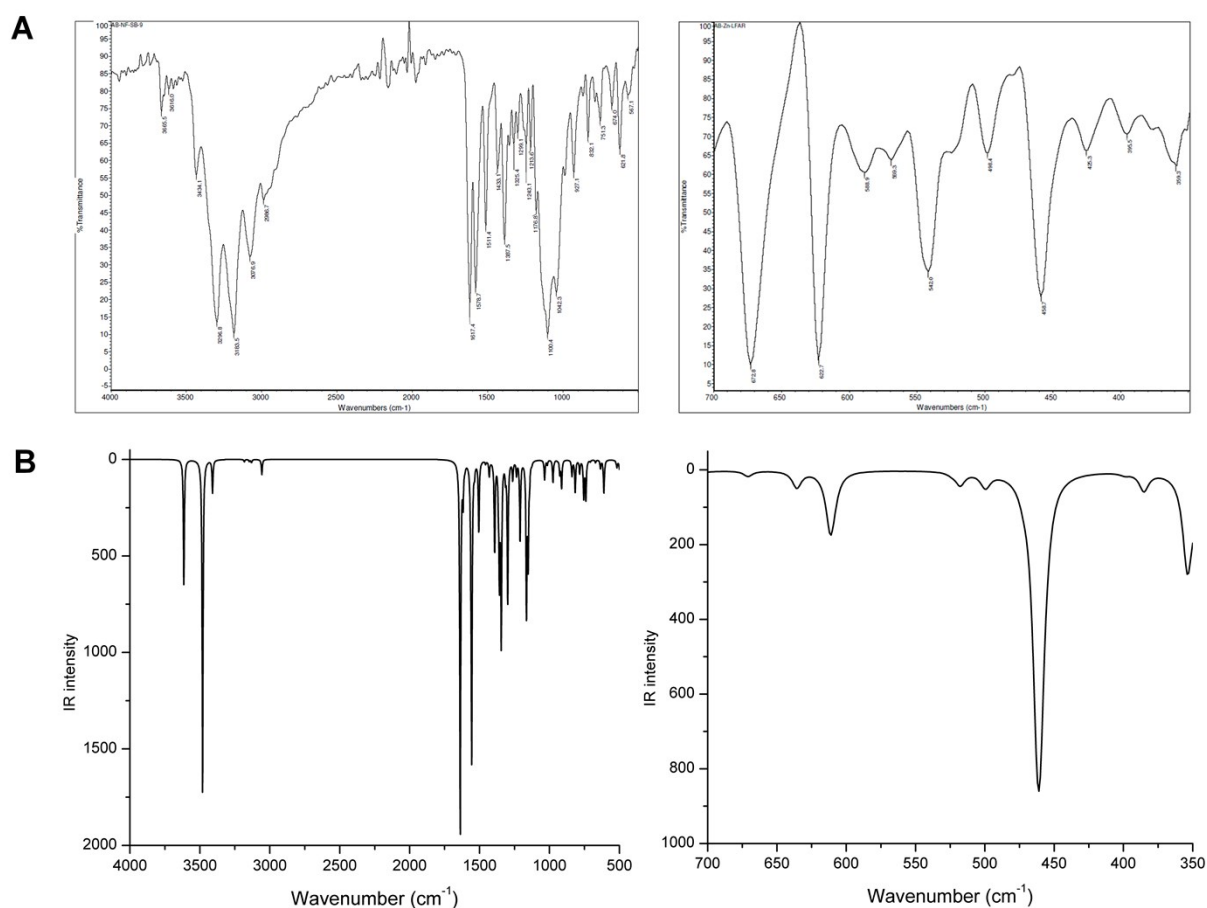
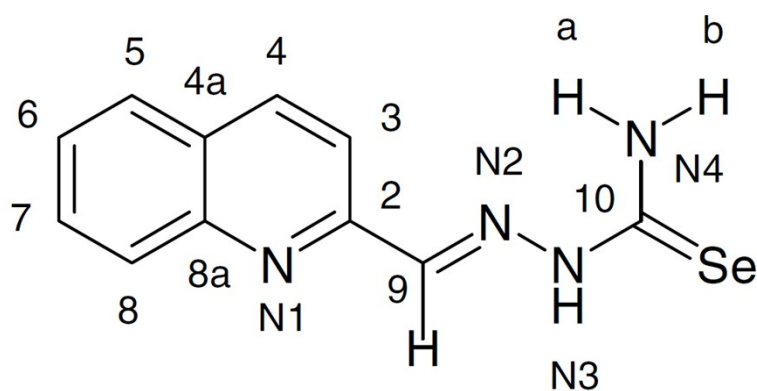


Figure S1. Experimental (A) and theoretical (B) FT-IR spectra of **1**.



Scheme S1. Numbering of atoms of Hqasesc in **1**, used in NMR.

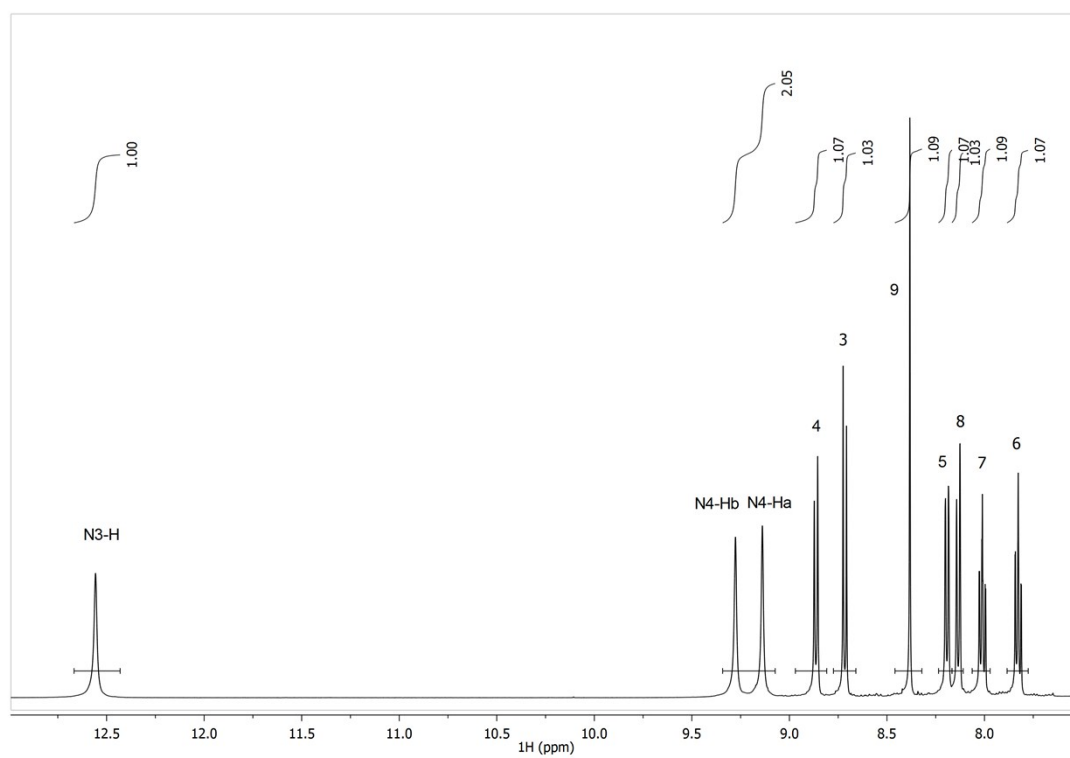


Figure S2. ^1H NMR spectrum of **1** in $\text{DMSO-}d_6$.

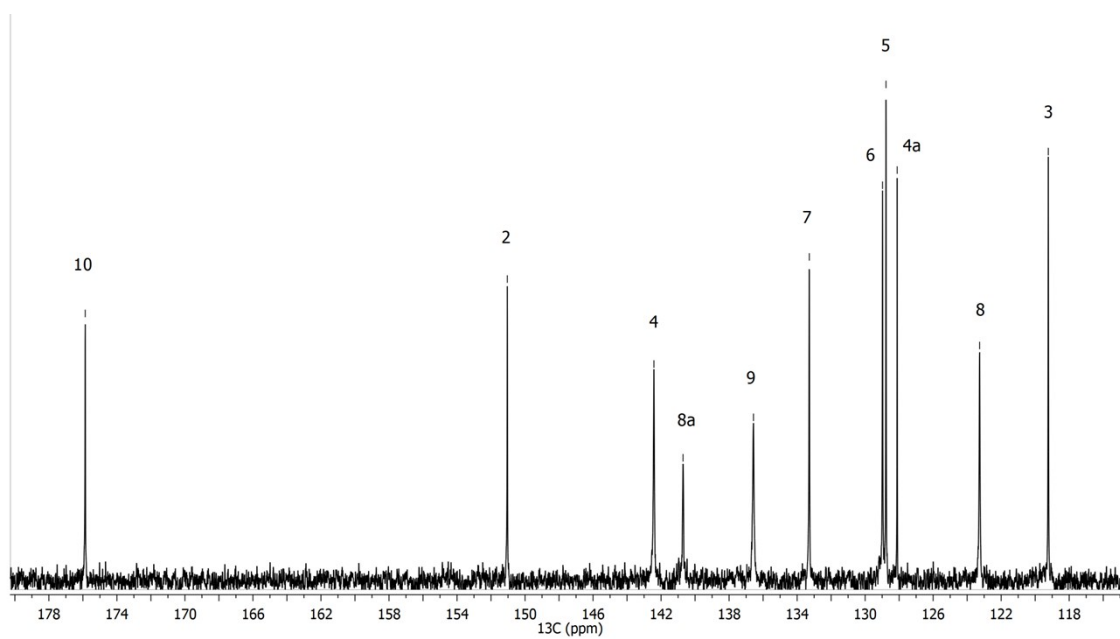


Figure S3. ^{13}C NMR spectrum of **1** in $\text{DMSO-}d_6$.

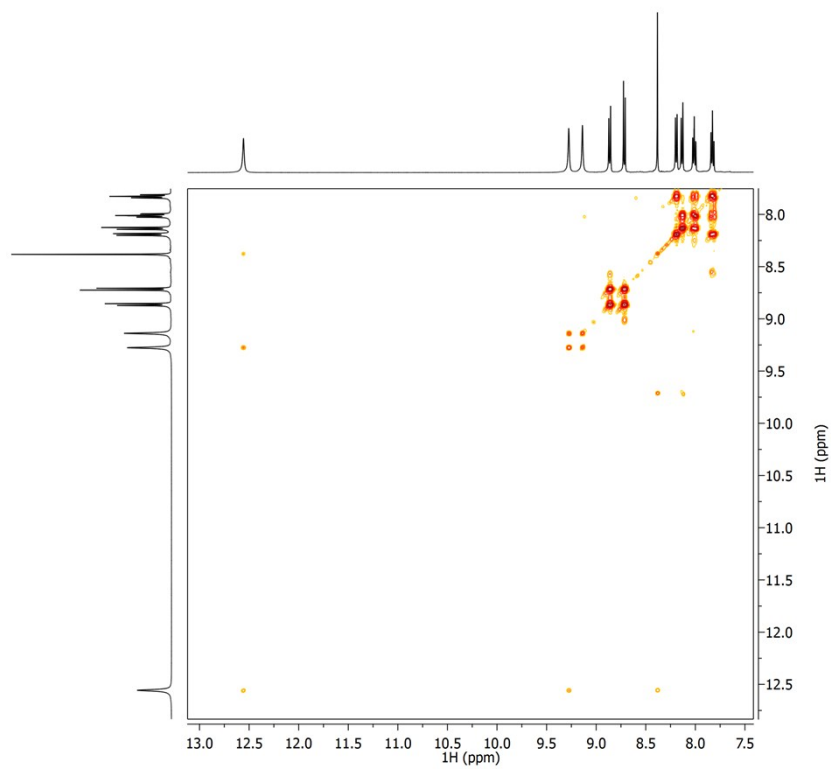


Figure S4. COSY spectrum of **1**.

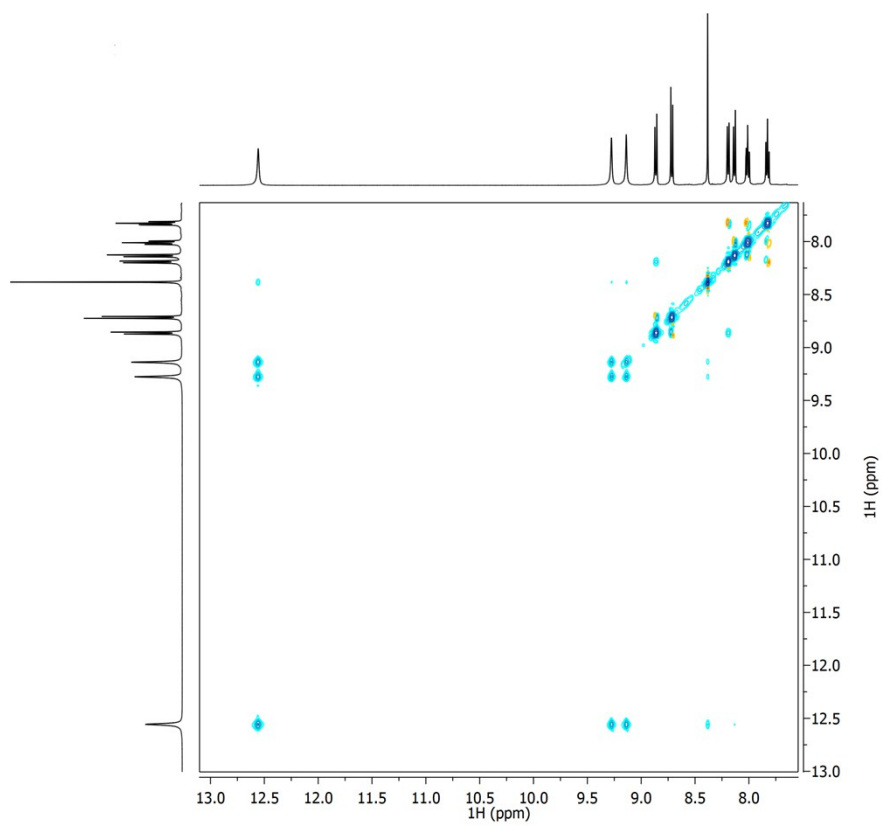


Figure S5. NOESY spectrum of **1**.

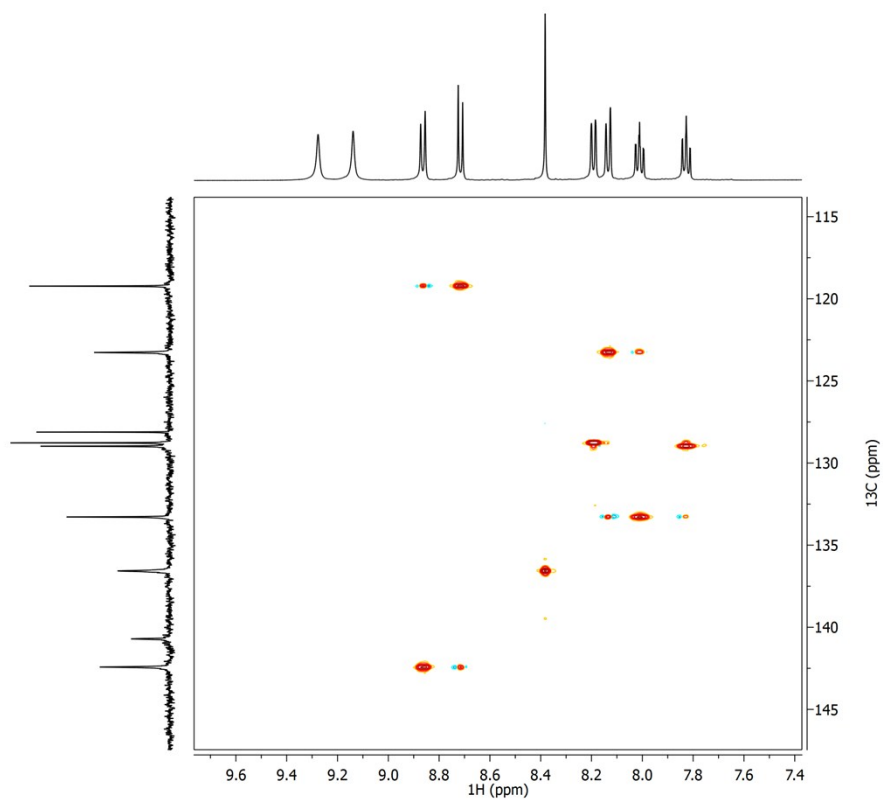


Figure S6. ^1H - ^{13}C HSQC spectrum of **1**.

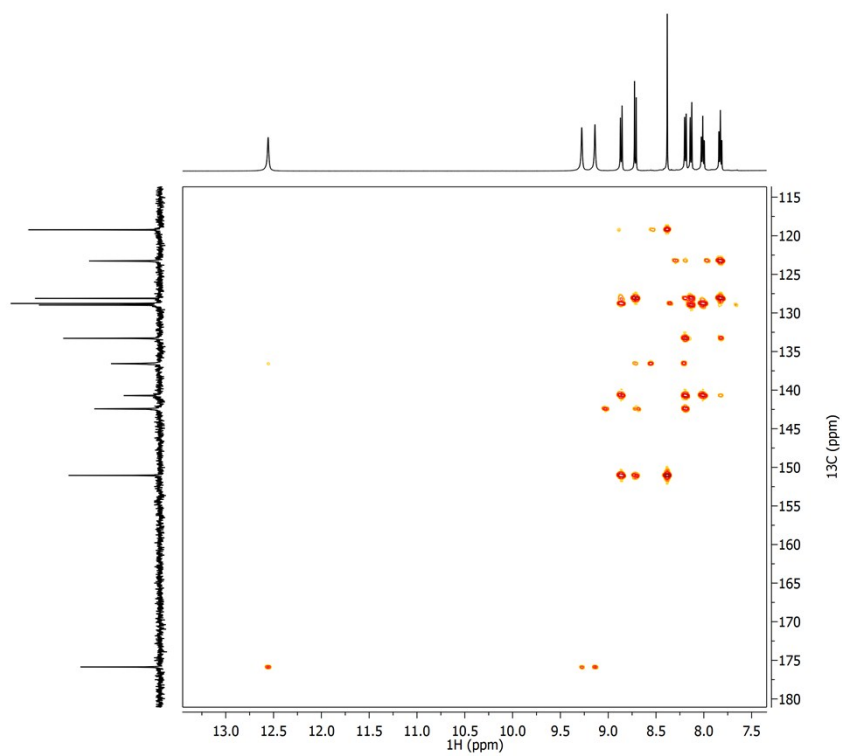


Figure S7. ^1H - ^{13}C HMBC spectrum of **1**.

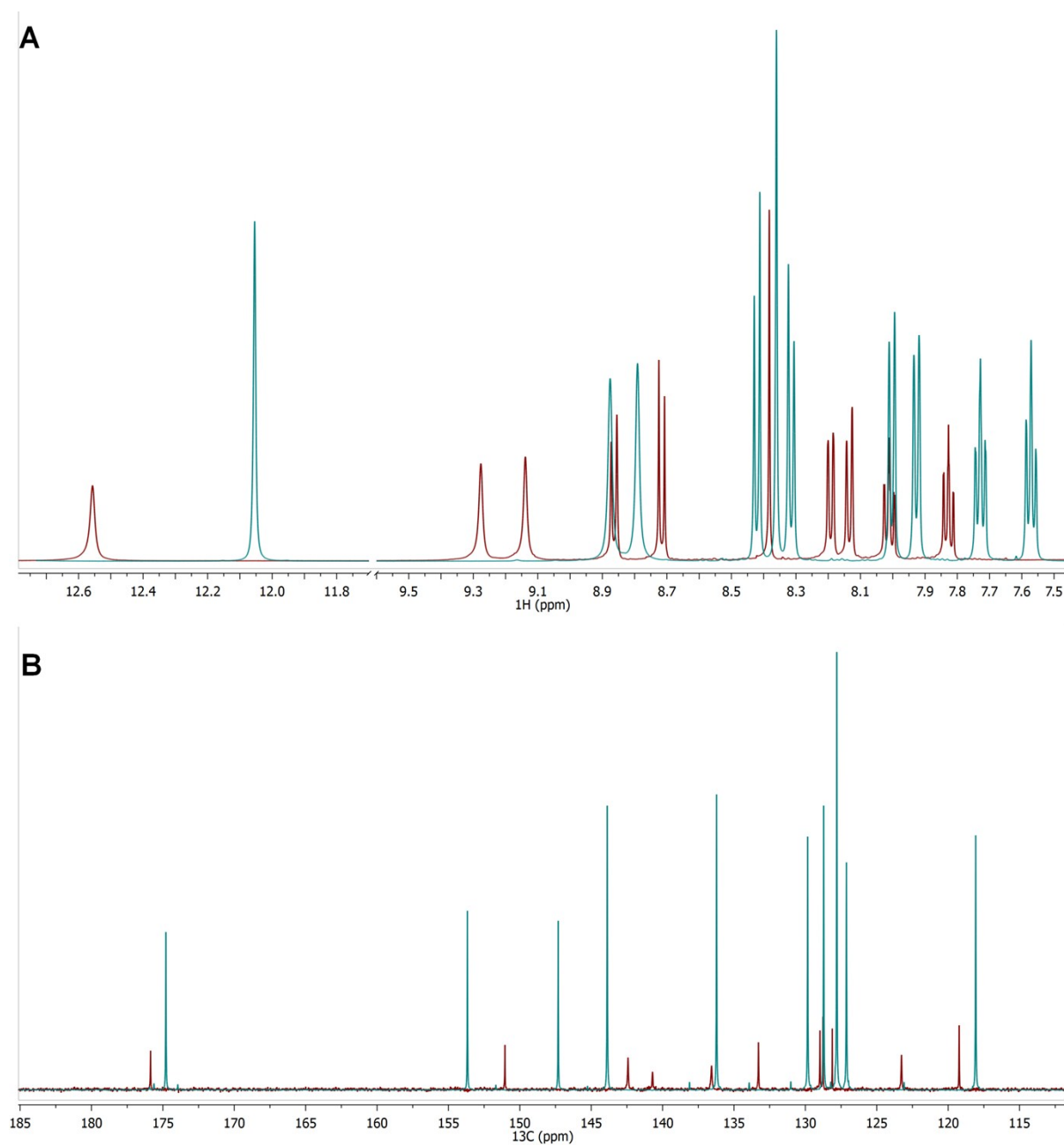


Figure S8. Superimposed ^1H (A) and ^{13}C NMR spectra (B) of Hqasesc (cyan) and **1** (red).

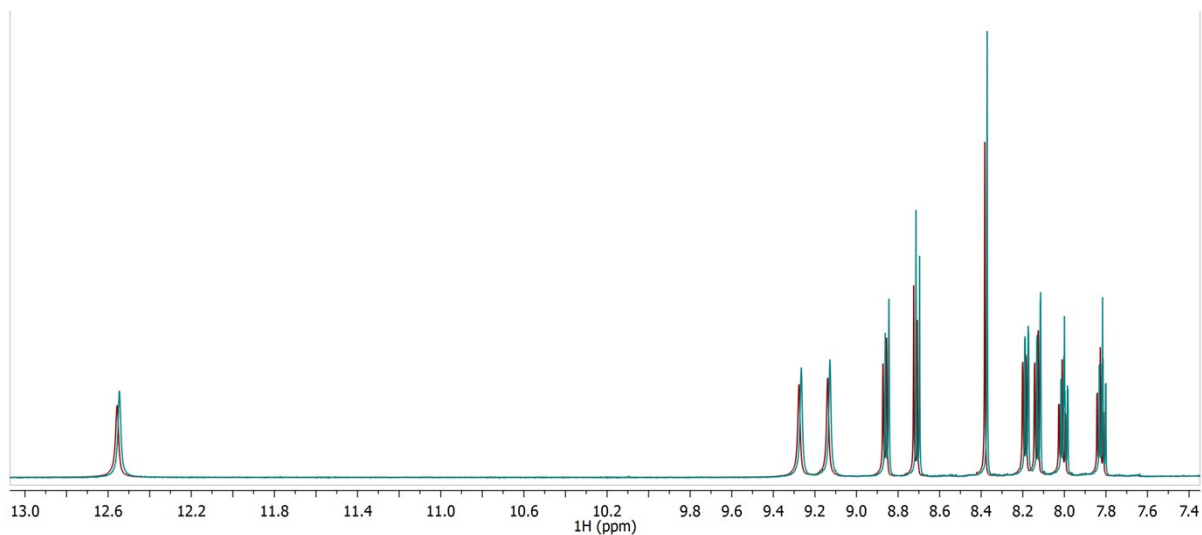


Figure S9. Superimposed ^1H NMR spectra of freshly prepared sample of **1** (cyan) and sample after 24 h (red).

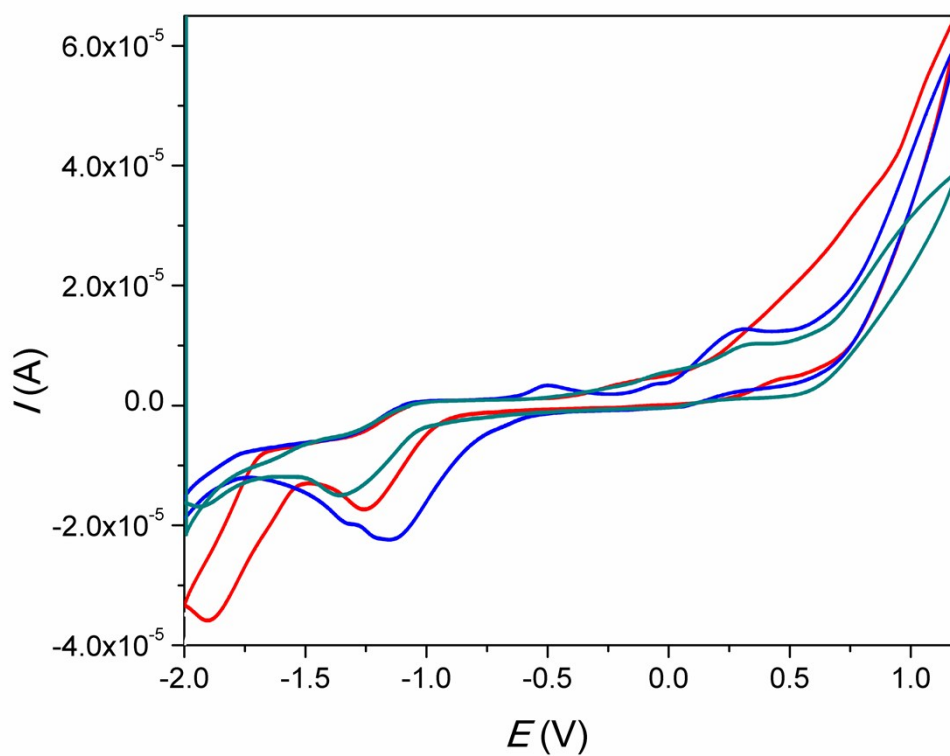


Figure S10. Cyclic voltammograms of Hqasesc (cyan), **1** (blue), and **1** with addition of zinc perchlorate (red) in anhydrous DMSO containing 0.10 M $[\text{n-Bu}_4\text{N}][\text{PF}_6]$ at a scan rate of 100 mV s^{-1} using a glassy carbon working electrode.

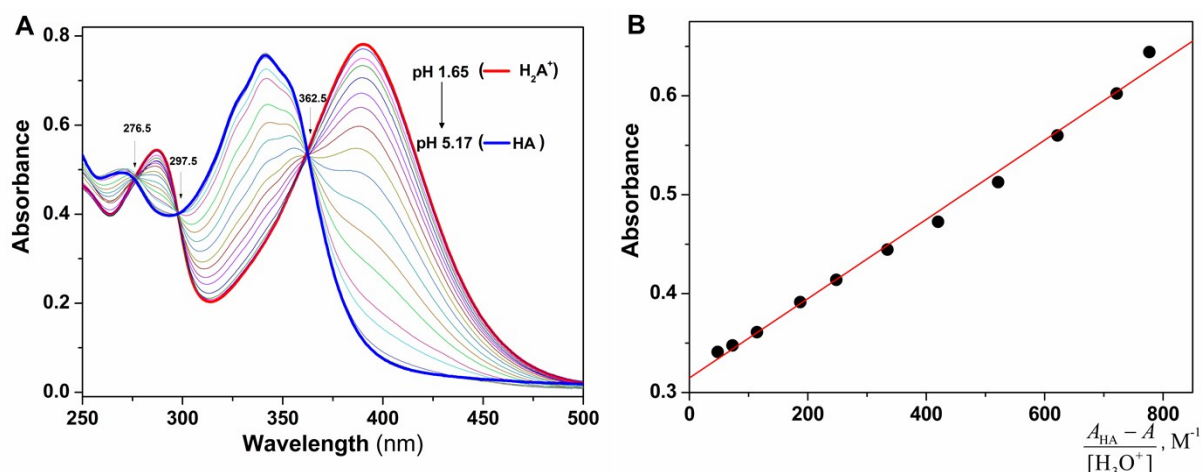


Figure S11. (A) UV-Vis spectra of Hqasesc in pH range 1.65–5.17 used for pK_{a1} determination ($t = 25\text{ }^{\circ}\text{C}$); The spectra were recorded at following pH values: 1.65, 1.83, 2.06, 2.46, 2.71, 3.03, 3.17, 3.33, 3.67, 3.84, 4.13, 4.30, 5.17; Spectra of pure H_2A^+ , and HA forms and isosbestic points are indicated. (B) Determination of K_{a1} at 341 nm according to equation 2; slope = 4.01×10^{-4} , intercept = 0.315, $r^2 = 0.993$.

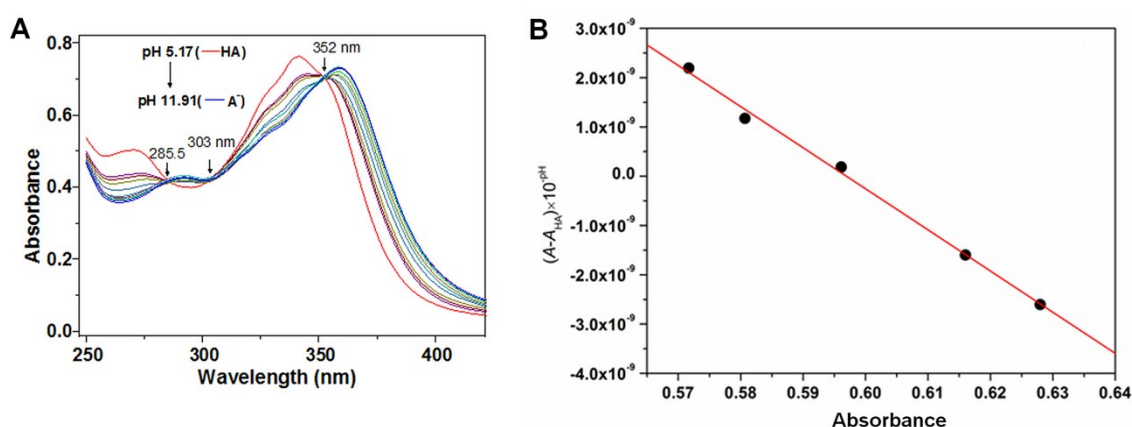


Figure S12. (A) UV/Vis Spectra of Hqasesc in pH range 5.17–11.91 used for pK_{a2} determination ($t = 25\text{ }^{\circ}\text{C}$); The spectra were recorded at following pH values: 5.17, 6.56, 7.01, 7.32, 7.65, 8.06, 8.82, 11.91; Spectra of pure HA and A^- forms and isosbestic points are indicated. (B) Determination of K_{a2} at 365 nm according to equation 3a; slope = -8.34×10^{-8} , intercept = 4.97×10^{-8} , $r^2 = 0.995$.

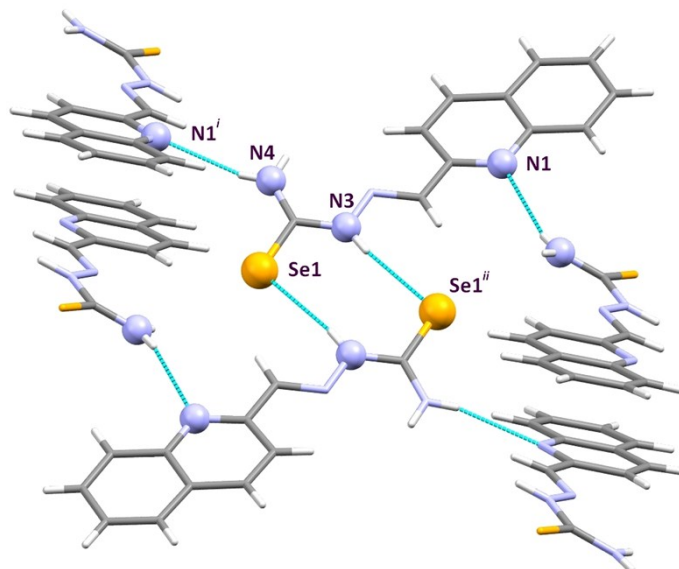


Figure S13. Packing diagram in the crystal structure of Hqasesc.

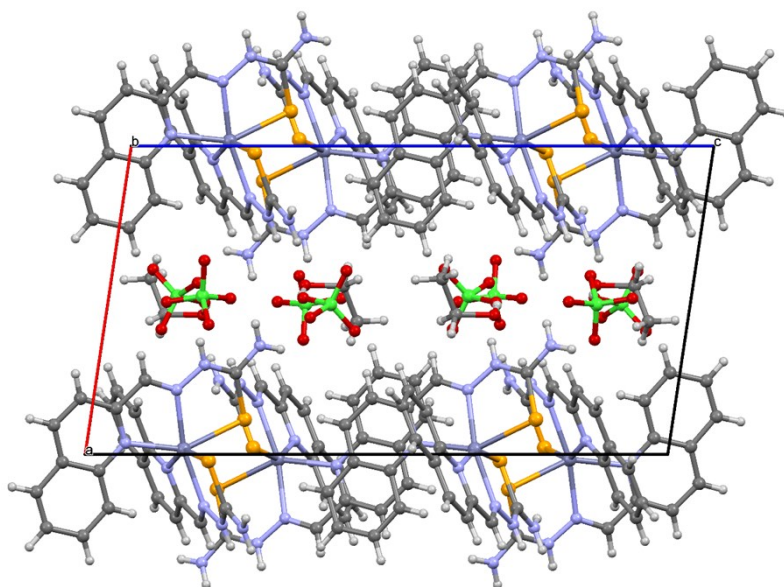


Figure S14. Packing diagram in the crystal structure of **1**.

Table S1. Hydrogen bonding geometry (Å, °) in Hqasesc and **1**.

$D-H\cdots A$	$D-H$	$H\cdots A$	$D\cdots A$	$D-H\cdots A$
Hqasesc				
N4–H4A \cdots N1 ⁱ	0.77(4)	2.45(4)	3.198(3)	163(3)
N3–H3 \cdots Se1 ⁱⁱ	0.86(3)	2.68(3)	3.533(2)	172(3)
1				
N3–H3 \cdots O3	0.866(18)	2.39(3)	3.082(4)	137(3)
N4–H4A \cdots O3	0.86	2.58	3.259(5)	137.1
N4–H4A \cdots O9A ⁱ	0.86	2.49	3.041(5)	122.7
N4–H4A \cdots O9B ⁱ	0.86	2.49	2.970(8)	116.3
N4–H4B \cdots O4 ⁱ	0.86	2.48	3.164(5)	137.3
N3A–H3A \cdots O9A ⁱⁱ	0.846(18)	2.01(2)	2.802(4)	155(4)
N3A–H3A \cdots O9B ⁱⁱ	0.846(18)	1.97(2)	2.795(7)	163(4)
N4A–H4C \cdots O7 ⁱⁱⁱ	0.86	2.34	3.017(5)	135.4
N4A–H4C \cdots O9A ⁱⁱ	0.86	2.35	3.085(5)	143.4
N4A–H4D \cdots Se1 ⁱⁱⁱ	0.86	2.67	3.447(3)	150.1
O9A–H9A1 \cdots O7 ^{iv}	0.82	2.19	2.955(8)	156.1
O9B–H9B \cdots O1	0.82	2.08	2.818(11)	150.1

Symmetry codes for Hqasesc: (i) $x - 1/2, -y + 3/2, z - 1/2$; (ii) $-x + 1, -y + 2, -z + 1$.
Symmetry codes for **1**: (i) $-x + 1, y + 1/2, -z + 1/2$; (ii) $-x, y + 1/2, -z + 1/2$; (iii) $-x, y - 1/2, -z + 1/2$; (iv) $x, y - 1, z$.

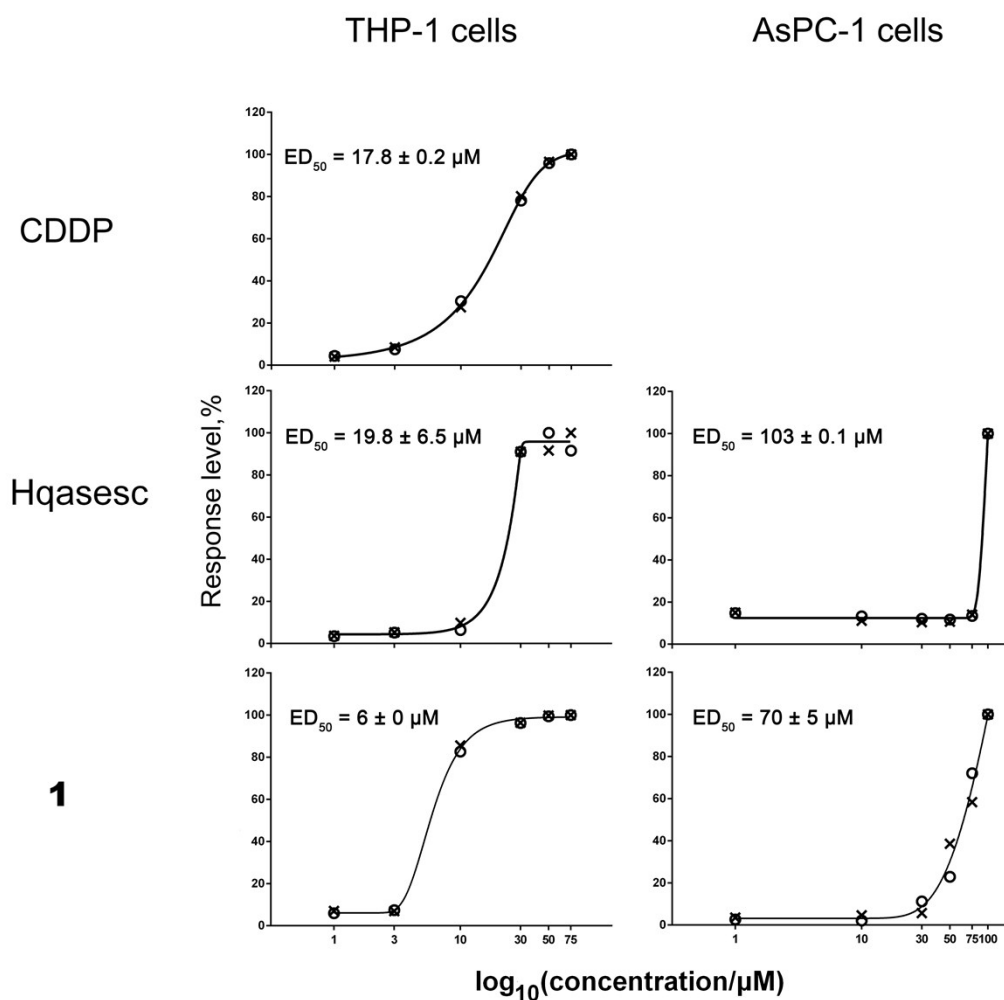


Figure S15. ED₅₀ values for Hqasesc, **1** and CDDP on THP-1 and AsPC-1 cells. THP-1 and AsPC-1 cells were treated with Hqasesc, **1** and CDDP applied in a range of six concentrations for 24 h, and afterwards stained with Annexin-V and PI. Percentages of all Annexin-V labeled cells for each concentration of investigated compounds were calculated as a proportion of the maximal apoptotic response normalized as 100%. Such scaled apoptotic outcomes were plotted against concentrations and ED₅₀ concentration was calculated using asymmetric sigmoidal curve five-parameter logistic equation (GraphPad Prism 6 software).

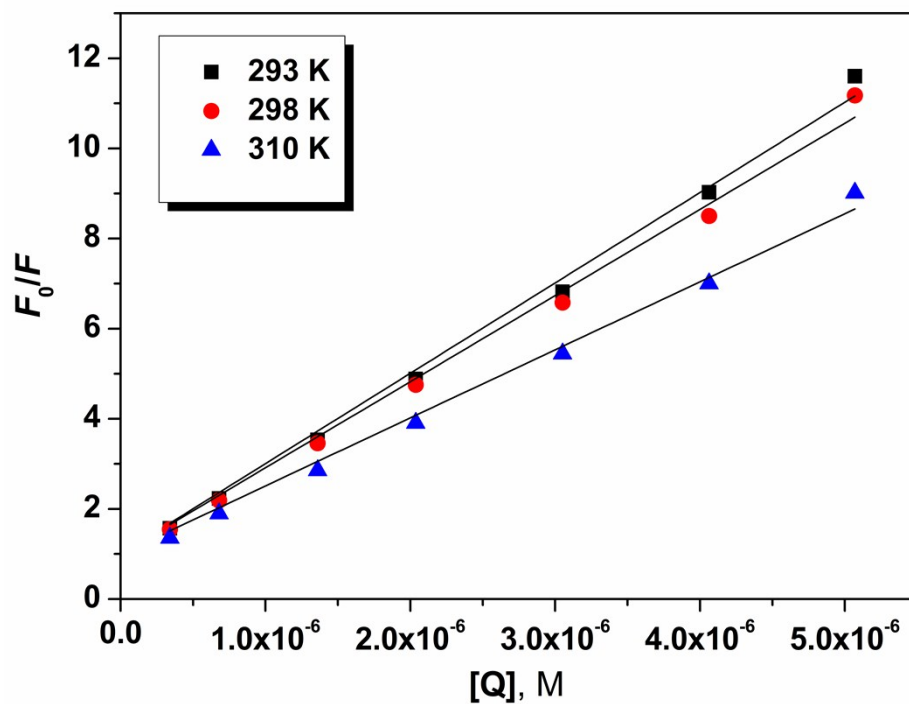


Figure S16. Stern-Volmer plot of F_0/F vs. $[Q]$ at three different temperatures, where F_0 and F represents HSA fluorescence intensities in absence (F_0) and in presence of the quencher (F), and $[Q]$ is the concentration of the quencher (**1**).

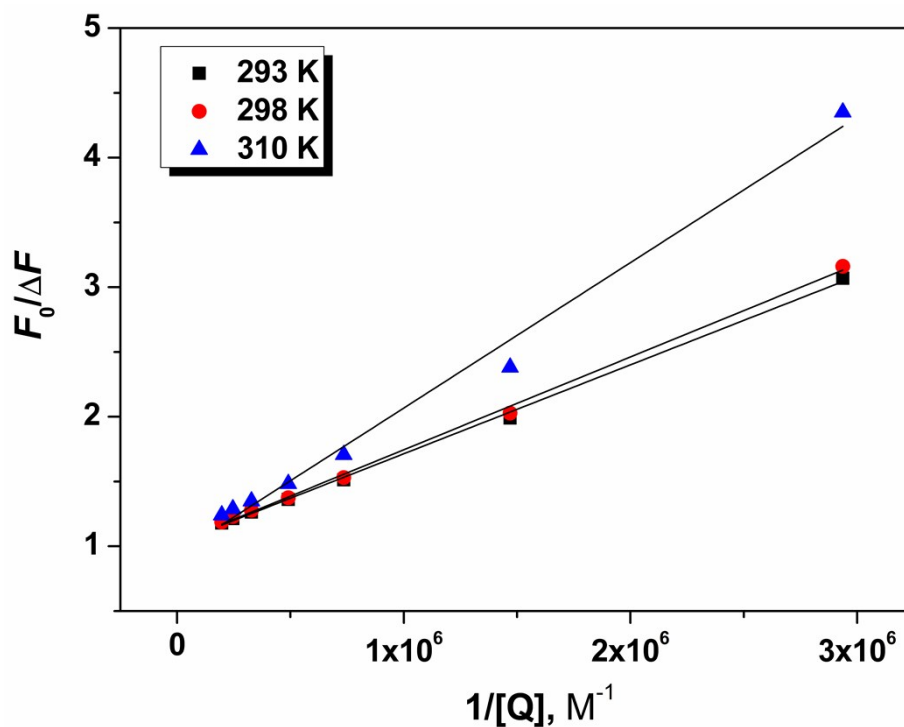


Figure S17. Modified Stern-Volmer plot for binding of **1** to HSA at three temperatures.

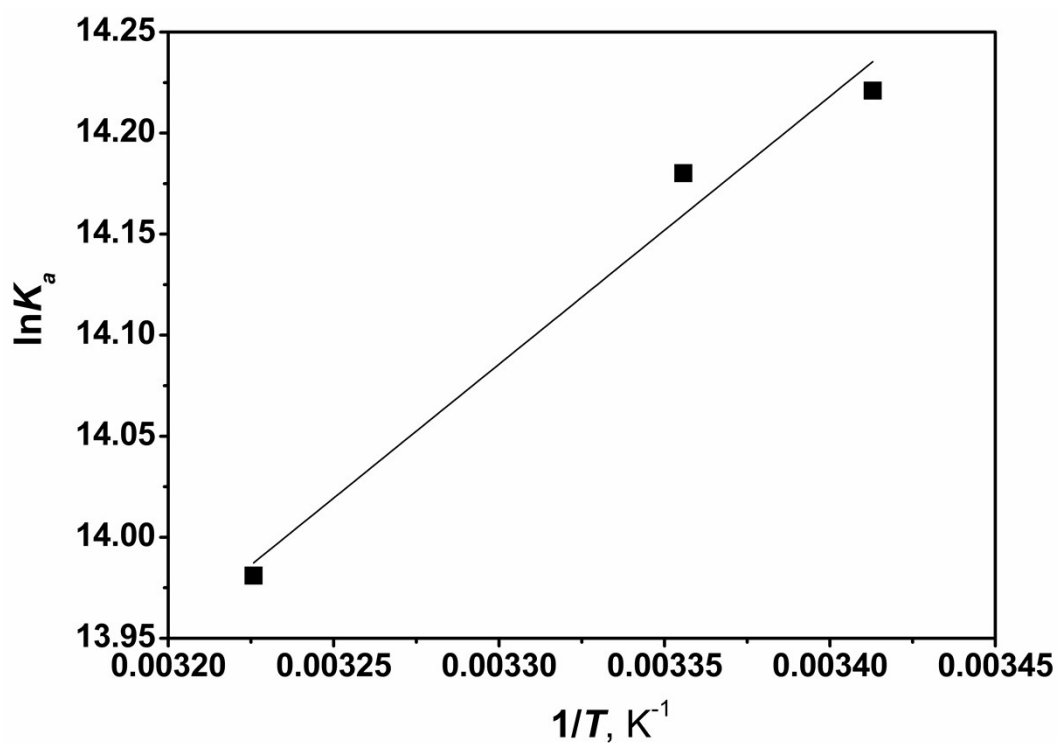


Figure S18. The plot of $\ln K_a$ (K_a given in M^{-1}) vs. $1/T$ for the interaction of **1** with HSA.

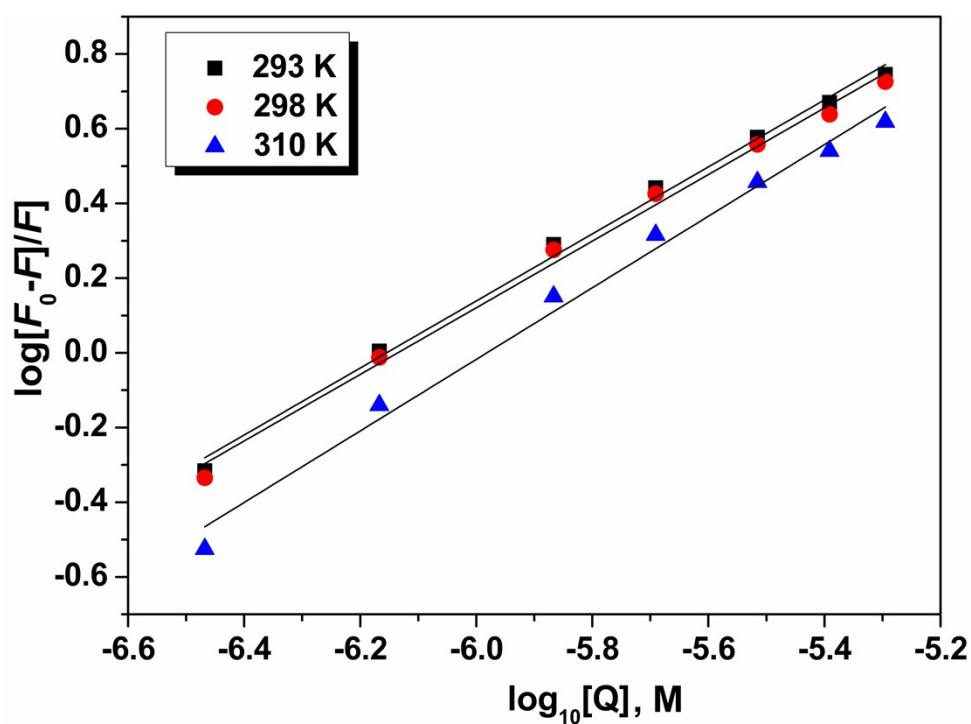


Figure S19. Double-log plot for determination of binding constants K_b , and the number of binding sites n at three temperatures; Concentration of quencher, $[Q]$ is given in M.

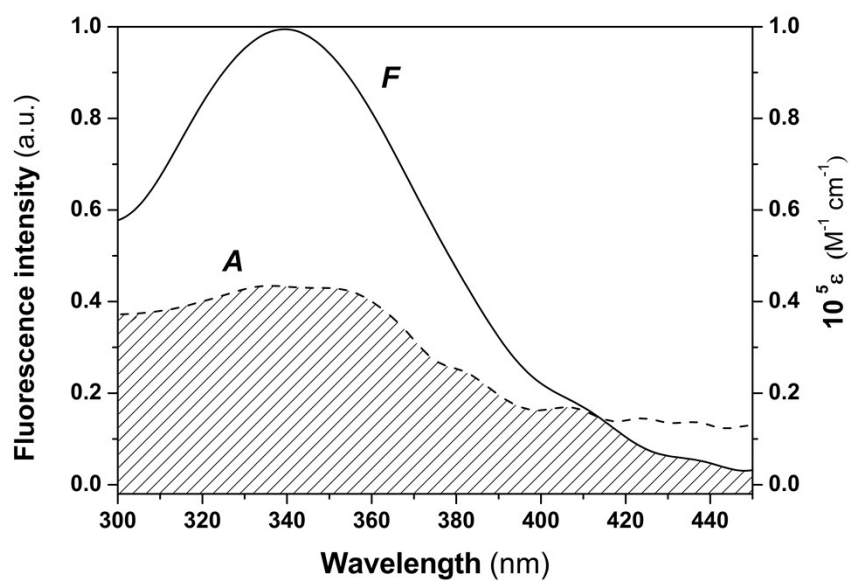


Figure S20. Spectral overlap of complex **1** absorption (curve *A*, dashed line) with HSA fluorescence emission (*F*, solid line); $c(\text{HSA}) = c(\mathbf{1}) = 5 \times 10^{-7} \text{ M}$; $T = 298 \text{ K}$.

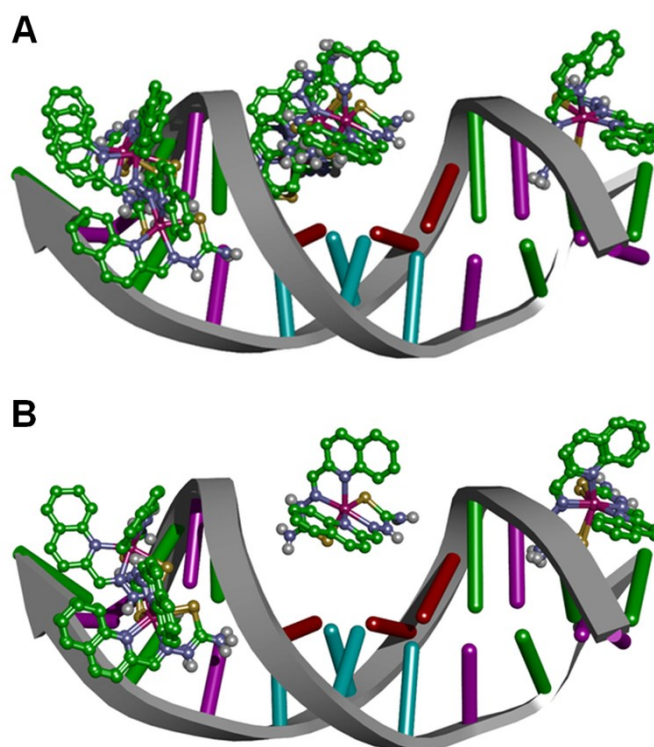


Figure S21. All conformations of complex **1** in the DNA duplex of sequence $\text{d}(\text{CGCGAATTCGCG})_2$ from PDB IDs 3U2N^{S1} (A) and 4U8A^{S2} (B).

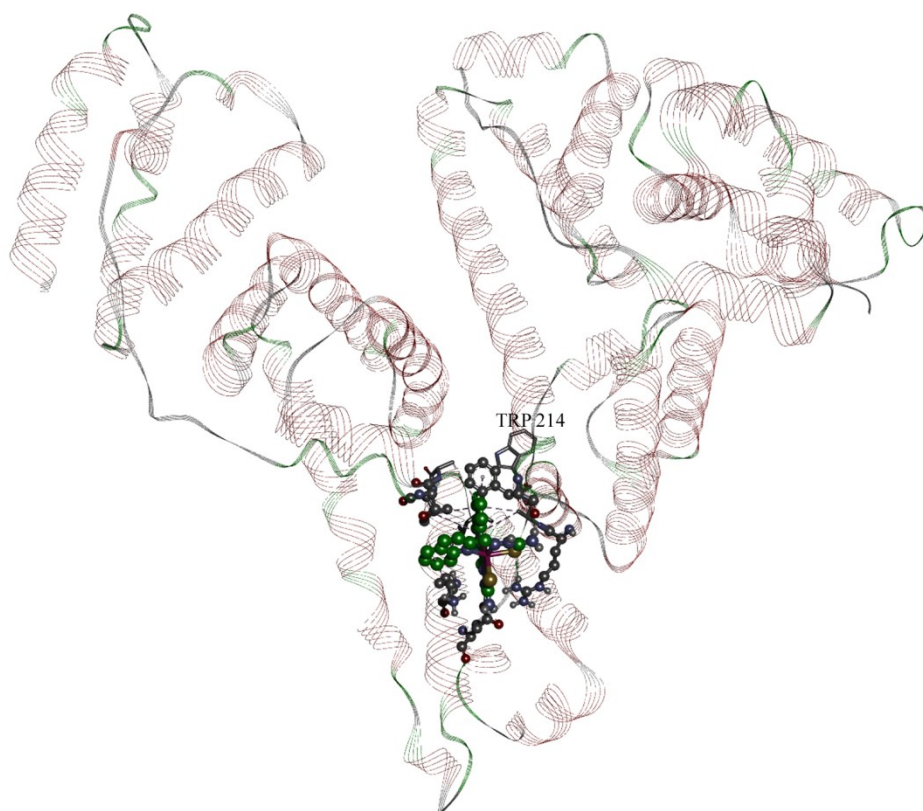


Figure S22. Structure of HSA (PDB ID 1BJ5^{S3}) and the location of complex 1 binding site.

Table S2. Interactions of HSA binding site atoms with **1**.

Residue (atom)	Interaction type	Distance
Glu 354 (OE1)	Hydrogen bond/electrostatic	2.089
Glu 354 (OE1)	Hydrogen bond/ electrostatic	2.726
Phe 206 (O)	Hydrogen bond	1.987
Ala 210	Hydrophobic CH- π	4.639
Ala 210	Hydrophobic CH- π	3.725
Leu 347	Hydrophobic CH- π	4.968
Lys 351	Hydrophobic CH- π	5.074
Leu 481	Hydrophobic CH- π	4.903
Val 482	Hydrophobic CH- π	4.814
Val 482	Hydrophobic CH- π	5.247
Phe 206	Hydrophobic / π - π	4.603
Arg 209 (NH1) – Se	Hydrogen bond	2.749

References

- S1 D.G. Wei, , W.D. Wilson and S. Neidle, *J. Am. Chem. Soc.*, 2013, **135**, 1369–1377.
- S2 W. Zhu, Y. Wang, K. Li, J. Gao, C.H. Huang, C.C. Chen, T.P. Ko, Y. Zhang, R.T. Guo and E. Oldfield, *J. Med. Chem.*, 2015, **58**, 1215–1227.
- S3 S. Curry, H. Mandelkow, P. Brick and N. Franks, *Nat. Struct. Biol.*, 1998, **5**, 827–835.